

# Enhancement of field generation via maximal atomic coherence prepared by fast adiabatic passage in Rb vapor

V. A. Sautenkov<sup>1,3</sup>, C. Y. Ye<sup>1</sup>, Y. V. Rostovtsev<sup>1</sup>, G. R. Welch<sup>1</sup>, and M. O. Scully<sup>1,2</sup>

<sup>1</sup>*Institute for Quantum Studies and Department of Physics,  
Texas A&M University, College Station, TX 77843*

<sup>2</sup>*Department of Chemistry, Princeton University, Princeton, NJ 08544*

<sup>3</sup>*Lebedev Institute of Physics, Moscow 117924, Russia*

(Dated: September 7, 2018)

We have experimentally demonstrated the enhancement of coherent Raman scattering in Rb atomic vapor by exciting atomic coherence with fractional stimulated Raman adiabatic passage. Experimental results are in good agreement with numerical simulations. The results support the possibility of increasing the sensitivity of CARS by preparing atomic or molecular coherence using short pulses.

PACS numbers: 32.80.Qk, 42.65.Dr, 42.50.Hz

Although four-wave mixing processes have been studied for at least twenty-five years [1, 2], it has only recently been shown that quantum coherence can dramatically increase the nonlinear response in atomic, molecular, or solid state media without overwhelming absorption [3, 4, 5, 6, 7]. Currently the subject of quantum coherence is the focus of broad research including quantum computing and quantum state storage [8, 9, 10], manipulation of single quanta [11, 12, 13]; in a coherently prepared medium with maximal coherence there occur effective frequency conversion [14, 15], sub-femtosecond pulse generation [16], and enhanced CARS spectroscopy [17].

Maximal coherence in atoms and molecules can be created with a pair of short coupling pulses which adiabatically interact with an atomic or molecular system as depicted in Fig. 1. By choosing the proper time dependence of the pulses shown in Fig. 1a, 100% population transfer between lower levels can be achieved. This is referred to as Stimulated Raman Adiabatic Passage, or STIRAP [18, 19]. However, using the time dependence shown in Fig. 1b, referred to as fractional STIRAP (to distinguish the technique from STIRAP) we can create maximal coherence between the lower levels.

In this Letter, we report an experimental implementation of fractional STIRAP in a Rb vapor cell near room temperature where lower level coherence is created between Zeeman sublevels. We demonstrate coherent Raman scattering in the Rb vapor using short laser pulses (shorter than the life-time of the excited state.) We observe enhancement of the coherent Raman scattering under the condition of maximal coherence between Zeeman sublevels prepared by fractional STIRAP. The observed intensity of the signal pulse depends quadratically on the density of Rb atoms. We theoretically predict this behavior, and show that the experiments are in agreement with numerical simulations.

The essence of the technique is the following. Two coupling pulses (with duration less than the life-time of the excited state) with Rabi frequencies  $\Omega_1$  and  $\Omega_2$  resonant with transitions  $a - c$  and  $a - b$  (see Fig. 1) create coherence be-

tween levels  $b$  and  $c$ . After some time, (less than the life-time of the lower level coherence) the probe pulse  $\Omega_3$  arrives and scatters from the atomic coherence  $\rho_{bc}$  leading to efficient generation of a signal field  $\Omega_4$ . The important points are that the frequency of the signal field is shifted exactly to the transition frequency between levels  $b$  and  $c$ , and the intensity of the signal field depends on the magnitude of the atomic coherence  $\rho_{bc}$ .

The main result of this Letter is shown in Fig. 2. By changing the time delay, one can see that there is a maximum of efficiency of generation of the signal field corresponding to the configuration of the coupling pulses that creates maximum coherence. It is this coherence that distinguishes the present technique from ordinary coherent anti-Stokes Raman spectroscopy (CARS) where the coherence level is low.

An important feature of our experiments that distinguishes them from prior experiments such as those on photon storage [8, 9, 10] is that the duration of the pulses are short in comparison with the relaxation rates of the associated optical transitions. Furthermore, in those experiments the magnitude of  $\rho_{bc}$  coherence was relatively low, and the duration of the pulses was long compared to the optical lifetime and comparable to the spin coherence lifetime. Note also that, because there is no inhomogeneous broadening of spin transition, our approach is different from the echo technique where the additional  $\pi$ -pulses to control spin coherence are applied [20].

Also our work is different from the work done by Harris group at Stanford where very efficient technique employing maximal atomic coherence was developed. Their duration of pulse is longer than the optical relaxation time (duration of the laser pulses is 15 ns, while  $T_1 = 5.2$  ns for level  $6p7s\ ^3P_1$  of  $^{208}Pb$ ). Thus, the laser field is practically quasi-stationary, and population of the dark state occurs via optical pumping rather than via rapid adiabatic passage. While in our experiments, we use a fractional STIRAP to create coherence between hyperfine levels, also the duration of pulses is shorter than population relaxation of the excited state. Us-

ing the regime of strong saturation regime gives one a very robust effect of coherence excitation between atomic levels.

A schematic diagram of the experimental setup is shown in Fig. 3. Radiation from an external-cavity diode laser is tuned to the  $D_1$  transition of  $^{87}\text{Rb}$   $5S_{1/2}$  ( $F = 2$ ) to  $5P_{1/2}$  ( $F' = 1$ ). The beam is split by a beam-splitter and passes through acousto-optic modulators (AOM) driven by pulses with adjustable duration and delay (the rise time of the AOM is near 9 ns), and the same frequency shift (200 MHz). The optical path lengths for both beams are the same. The temporal behavior of the pulses is detected by fast photodiode  $D_3$ .

One beam serves as the first coupling pulse and the probe pulse. The time duration of the first coupling pulse is 150 ns, and that of the second pulse is 20 ns. The other beam, also of 20 ns duration, is used as the second coupling pulse. Front and tail slopes of the pulses are limited by the AOMs and are synchronized electronically. The polarization of the first beam (which includes the first coupling pulse and the probe pulse) is rotated by  $90^\circ$  relative to the polarization of the other pulse. These orthogonally polarized laser beams are combined by a polarizing beam-splitter.

The polarization of the pulses is modified by a  $\lambda/4$  wave-plate, which results in opposite circular polarization of the two pulses. The combined laser beams are focused by a lens (focus length 30 cm) into a cell of length 2.5 cm containing saturated Rb vapor with atomic density  $N = 1 \times 10^{11} \text{ cm}^{-3}$ . The cell is installed in a three-layer magnetic shield. The atomic density is estimated from the temperature of the cell and corrected by absorption measurements [21]. After the cell, the transmitted laser beams with opposite circular polarizations are separated by a second  $\lambda/4$  wave-plate and another polarizing beam splitter. The transmitted first coupling pulse and probe pulse are detected by fast photodiode  $D_1$ . The second coupling pulse and the generated signal pulse are detected by fast photodiode  $D_2$ . All fast photodiodes have identical characteristics with 1 ns resolution.

The coupling pulses create ground state coherence in the atomic vapor. Then after some time delay, the pulse of probe field scatters on the atomic coherence to generate of a new field (signal). Three different temporal combinations of the coupling pulses and the probe pulse are shown in Fig. 4.

The energy of the first coupling pulse is 375 pJ, its duration is 150 ns that was selected so that several optical pumping cycles can occur before the second coupling pulse is applied. The time delay between the end of the first coupling pulse and the probe pulse is 100 ns, which is considerably less than the ground state coherence decay time of about  $10^3$  ns, and more than three times longer than the excited state lifetime. The energy of the second coupling pulse is 50 pJ, and its duration of 20 ns that is short enough to perform STIRAP for the time period less than the life time of excited state (27 ns). Effective area of the laser beams is about  $2 \times 10^{-3} \text{ cm}^2$ ; corresponding Rabi frequency for every beam is  $\Omega = 10\gamma$  (where  $\gamma = 1/\tau$  and  $\tau = 27$  ns), so we fulfilled the condition  $\tau\sqrt{\Omega_1^2 + \Omega_2^2} \geq 10$  (see in Ref.[18] for details).

Figure 5 shows the probe and signal fields after their propagation through the cell. The combination of coupling pulses shown in Fig. 4a and 4c is not optimal for a large ground-state coherence to remain after the pulses are gone. As a result, the corresponding signal fields in Fig. 5a and 5c have small amplitudes. The optimal signal (with maximum amplitude) shown in Fig. 5b is obtained by adjusting the time delay of the second coupling pulse relative to the first coupling pulse in such a way that the condition for fractional STIRAP is fulfilled. In this case, fractional STIRAP induces ground state coherence which is expected to be close to the maximal coherence. The amplitude of the generated field is 0.37 of the amplitude of the initial probe pulse.

Figure 2 shows the normalized amplitude of the generated new field (signal) as a function of delay time between coupling pulses for three different densities  $N = (1; 0.8; 0.4) \times 10^{11} \text{ cm}^{-3}$ . Zero time delay corresponds the situation where the tails of the first and second coupling fields switched off simultaneously. This is the condition for obtaining effective fractional STIRAP and maximal coherence. One can see that the efficiency is proportional to the square of the atomic density.

To gain physical insight into this process, we have performed numerical simulations for the propagation of the laser pulses in the medium. Instead of the real physical energy level manifolds ( $5S_{1/2}(F = 2) \leftrightarrow 5P_{1/2}(F' = 1)$  transition) we base our calculations on an idealized three level system as depicted in Fig. 1a. The experiments are done near room temperature, so we assume that the ground states are equally populated before the coupling pulses are applied.

Consider a three-level system selectively coupled by three laser pulses. The first two are coupling pulses, and the third is a probe pulse. The two coupling fields,  $\varepsilon_1$  and  $\varepsilon_2$ , with Rabi frequency  $\Omega_1$  and  $\Omega_2$ , respectively, excite transitions  $a \rightarrow c$  and  $a \rightarrow b$ . This generates coherence between levels  $b$  and  $c$ . Somewhat later, the probe pulse  $\varepsilon_3$ , with Rabi frequency  $\Omega_3$ , interacts with the medium. Because the medium already has coherence  $\rho_{bc}$ , coherent Raman scattering of the probe pulse leads to the generation of a signal pulse  $\varepsilon_4$  with Rabi frequency  $\Omega_4$ .

The interaction Hamiltonian in the rotating wave approximation for this system is

$$H = -\hbar \left( \sum_{ij} \Omega_{ij} |i\rangle \langle j| + h.c. \right) - \hbar \sum_j \Delta_j |j\rangle \langle j|, \quad (1)$$

where  $\Omega_{ij} = \wp_{ij} \varepsilon_{ij} / \hbar$  is the Rabi frequency of the respective fields,  $\wp_{ij}$  is the electrical dipole matrix element between states  $i$  and  $j$ ,  $\varepsilon_{ij}$  is the amplitude of the respective laser field, and  $\Delta_j$  is the laser detuning from the atomic resonance. The time-dependent density matrix equations of motion are

$$\frac{\partial \rho}{\partial \tau} = -\frac{i}{\hbar} [H, \rho] - \frac{1}{2} (\Gamma \rho + \rho \Gamma), \quad (2)$$

where  $\Gamma$  is the decay operator, and  $\rho$  is the atomic density matrix. Solving these equations gives the time evolution of the density matrix. To form a self-consistent system of

equations, one should add an equation for field propagation which is given by

$$\frac{\partial \varepsilon_{ij}}{\partial \xi} = -i\eta\rho_{ij}(\xi, \tau), \quad (3)$$

where  $\varepsilon_{ij}$  is the Rabi frequency of the field that is coupled to transition  $i \leftrightarrow j$ ,  $\rho_{ij}$  is the coherence between levels  $i$  and  $j$ ,  $\eta = \nu N \varphi_{ij} / (2\epsilon_0 c)$  is a coupling constant,  $\nu$  is the frequency of the field,  $N$  is the density of medium,  $\epsilon_0$  is the permittivity of the vacuum, and  $c$  is the speed of light in vacuum. We use coordinates  $\xi$  and  $\tau$  which are related to the laboratory coordinates by  $\xi = z$  and  $\tau = t - z/c$ .

We performed numerical simulations of the above theory using the same values of the parameters as in the experiments. The results of these simulations are shown in Fig. 2(solid curve). Experimental and theoretical curves show similar behavior except in the wings, and small differences are seen in the maxima. Residual signal at large delay time can be associated with the long tails of pulses and residual CW background of the optical fields.

We have also studied the power dependence of the generation of the signal field. The total power of the pulses was reduced by variable attenuator installed before the first beam-splitter. The conversion efficiency varies only slightly for large changes in power (from our maximum level to half) and then decreases very rapidly as power is further reduced. These measurements confirms that we have enough power for STIRAP. The good agreement between our experimental and theoretical results confirms that we have indeed obtained maximal coherence via fractional STIRAP and observed enhanced time delayed stimulated Raman scattering with high efficiency. Fractional STIRAP is a robust technique to obtain maximum Raman scattering. We would like to note that we have also studied delayed Raman scattering at higher Rb densities, but we cannot obtain efficiency more than 0.4 due to the strong absorption and optical pumping to the other hyperfine level ( $F = 1$ ).

The results of our experiment support a femtosecond adaptive spectroscopic technique for coherent anti-Stokes Raman spectroscopy (FAST CARS) that has been recently suggested [17]. The technique takes advantage of maximum coherence induced between lower atomic or molecular vibrational levels. Several methods can be used for effective preparation of atomic coherence [17], such as coherent population trapping [22], chirped pulses, and the fractional STIRAP [23] which we use in this experiment. These results constitute the the first experimental evidence that the FAST CARS technique can be realized.

Note that FAST CARS is a universal technique which can be applied to either atoms or molecules in various environments (gas, liquid, and solids) and can be used in a practical time scale. Another important feature of FAST CARS is that it is capable of determining vibrational frequencies in one laser pulse. That is significantly different from ordinary CARS where the frequency of signal field is determined by the four-photon resonance, and tuning the coupling frequency is essential to determine the splitting of the levels.

In FAST CARS, the atomic coherence created by the first pair of pulses is oscillating at the frequency difference of the lower levels, and, after some time delay, an anti-Stokes signal appears as scattering from the probe pulse. Thus, the frequency shift between the probe and signal fields is exactly the splitting between the  $b$  and  $c$  levels.

In summary, we have implemented fractional STIRAP in a Rb vapor cell to generate maximum coherence between Zeeman sublevels. We have theoretically predicted and experimentally demonstrated coherent Raman scattering using short laser pulses (shorter than the relaxation of lifetime of excited state). We observe an enhancement of coherent Raman scattering under the condition of maximal coherence prepared by fractional STIRAP in agreement with the numerical simulations. The observed intensity of the signal pulse depends quadratically on the density of Rb atoms. These results support the idea of a FAST CARS technique utilized in a femtosecond time scale in order to improve sensitivity of CARS measurements and can be applied to various atomic, molecular, and biological systems.

We thank K.K. Lehman, R. Lucht, A.B. Matsko, S.E. Harris, P.R. Hemmer, W.S. Warren for useful discussions and gratefully acknowledge the support from the Office of Naval Research, the Air Force Research Laboratory (Rome, NY), Defense Advanced Research Projects Agency-QuST, Texas A&M University Telecommunication and Information Task Force (TITF) Initiative, and the Robert A. Welch Foundation.

- 
- [1] R. W. Boyd, *Nonlinear optics* (Boston, Academic Press, 1992).
  - [2] Y. R. Shen, *The principles of nonlinear optics* (New York, J. Wiley, 1984).
  - [3] S. E. Harris, G. Y. Yin, M. Jain, and A. J. Merriam, *Philos. Trans. R. Soc., London, Ser. A* **355** (1733), 2291 (1997).
  - [4] A. J. Merriam, S. J. Sharpe, M. Shverdin, D. Manuszak, G. Y. Yin, and S. E. Harris, *Phys. Rev. Lett.* **84**, 5308 (2000).
  - [5] H. Wang, D. Goorskey, M. Xiao, *Phys. Rev. Lett.* **87**, 073601 (2001).
  - [6] A.V. Turukhin, V.S. Sudarshanam, M.S. Shahriar, et al. *Phys. Rev. Lett.* **88**, 023602 (2002).
  - [7] A. B. Matsko, O. Kocharovskaya, Y. Rostovtsev, G. R. Welch, A. S. Zibrov, M. O. Scully, *The advances in Atomic, Molecular, and Optical Physics* **46**, 191 (2001), edited by B. Bederson and H. Walther.
  - [8] C. Liu, Z. Dutton, C. H. Behroozi, and L. V. Hau, *Nature (London)* **409**, 490 (2001).
  - [9] D. F. Phillips, A. Fleischhauer, A. Mair, R. L. Walsworth, M. D. Lukin, *Phys. Rev. Lett.* **86**, 783 (2001).
  - [10] A. S. Zibrov, A. B. Matsko, O. Kocharovskaya, Y. V. Rostovtsev, G. R. Welch, and M. O. Scully, *Phys. Rev. Lett.* **88**, 103601 (2002).
  - [11] S. E. Harris and Y. Yamamoto, *Phys. Rev. Lett.* **81**, 3611 (1998).
  - [12] S. E. Harris and L. V. Hau, *Phys. Rev. Lett.* **82**, 4611 (1999).
  - [13] M. D. Lukin and A. Imamoglu, *Phys. Rev. Lett.* **84**, 1419 (2000).

- [14] M. Jain, H. Xia, G. Y. Yin, A. J. Merriam, and S. E. Harris, *Phys. Rev. Lett.* **77**, 4326 (1996).
- [15] K. Hakuta, L. Marmet, and B. P. Stoicheff, *Phys. Rev. A* **45**, 5152 (1992).
- [16] S. E. Harris and A. V. Sokolov *Phys. Rev. Lett.* **81**, 2894 (1998).
- [17] M. O. Scully, G. W. Kattawar, P. R. Lucht, T. Opatrny, H. Pilloff, A. Rebane, A. V. Sokolov, and M. S. Zubairy, *Proc. Nat. Acad. Sci. (USA)* **9**, 10994 (2002).
- [18] N. V. Vitanov, M. Fleischhauer, B. W. Shore, K. Bergmann, *The advances in Atomic, Molecular, and Optical Physics* **46**, 55 (2001), edited by B. Bederson and H. Walther.
- [19] R. Netz, A. Nazarkin, and R. Sauerbrey, *Phys. Rev. Lett.* **90**, 063001 (2003).
- [20] A.E. Johnson, E.S. Maniloff, T.W. Mossberg, *Opt. Lett.* **24**, 1526 (1999).
- [21] V. A. Sautenkov, M. M. Kash, V. L. Velichansky, and G. R. Welch, *Laser Physics* **9**, 1 (1999).
- [22] E. Arimondo, in *Progress in Optics*, edited by E. Wolf (Elsevier Science, Amsterdam, 1996), p. 257.
- [23] R. Buffa, M. P. Anscombe, and J. P. Marangos, *Phys. Rev. A* **67**, 033801 (2003).

FIG. 1: (a) STIRAP. “Counter-intuitive” pulse sequence transfers population from level  $b$  to  $c$  with 100% efficiency. (b) Fractional STIRAP. A pair of pulses with the same back edge distributes populations equally and excites maximal coherence between levels  $b$  and  $c$ . The coherence between levels is depicted by triangles. (c) Applying  $\Omega_1$  and  $\Omega_2$  to a three-level atom, one can excite maximal Zeeman coherence via fractional STIRAP. Field  $\Omega_4$  is generated via coherent scattering of probe field  $\Omega_3$ .

FIG. 2: Efficiency of generation of field  $\Omega_4$  versus mutual delay between coupling pulses for three different atomic densities. Zero delay was selected for the condition where the tails of the pulses coincide. Experimental results (dotted curve). Results of numerical simulations (solid curve).

### Figure Caption

FIG. 3: Experimental setup.

FIG. 4: Experimental pulse shapes recorded before propagation of the optical fields through the Rb cell. The noise level in these data is due to the electronics.

FIG. 5: Probe and generated signal fields after propagation through atomic vapor. In all figures, the probe field is stronger than the signal field. Amplitudes are normalized to amplitude of the probe pulse before entering the cell. Fig. 5b demonstrates the maximal amplitude of the generated signal field obtained by the combination of preparation pulses shown in Fig. 4b.

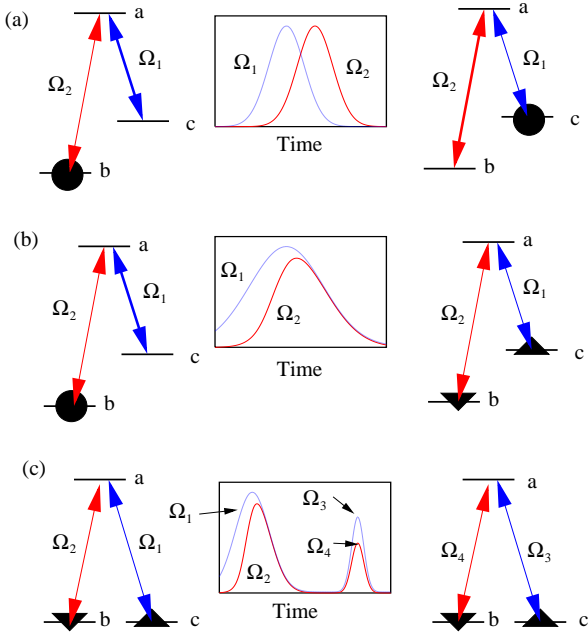


FIG. 1: (a) STIRAP. “Counter-intuitive” pulse sequence transfers population from level  $b$  to  $c$  with 100% efficiency. (b) Fractional STIRAP. A pair of pulses with the same back edge distributes populations equally and excites maximal coherence between levels  $b$  and  $c$ . The coherence between levels is depicted by triangles. (c) Applying  $\Omega_1$  and  $\Omega_2$  to a three-level atom, one can excite maximal Zeeman coherence via fractional STIRAP. Field  $\Omega_4$  is generated via coherent scattering of probe field  $\Omega_3$ .

Sautenkov et al., “Enhancement of field generation via maximal atomic coherence..”, Fig. 1.

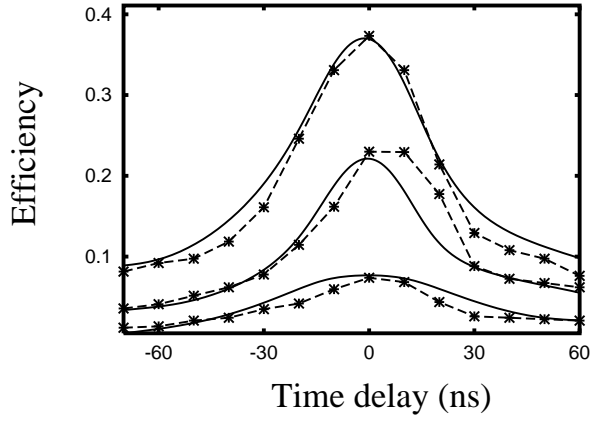


FIG. 2: Efficiency of generation of field  $\Omega_4$  versus mutual delay between coupling pulses for three different atomic densities. Zero delay was selected for the condition where the tails of the pulses coincide. Experimental results (dotted curve). Results of numerical simulations (solid curve).

Sautenkov et al., “Enhancement of field generation via maximal atomic coherence..”, Fig. 2.

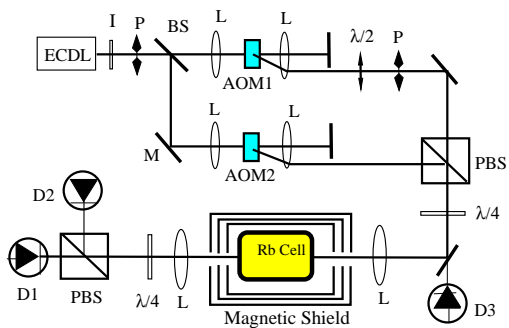


FIG. 3: Experimental setup.

Sautenkov et al., “Enhancement of field generation via maximal atomic coherence..”, Fig. 3.



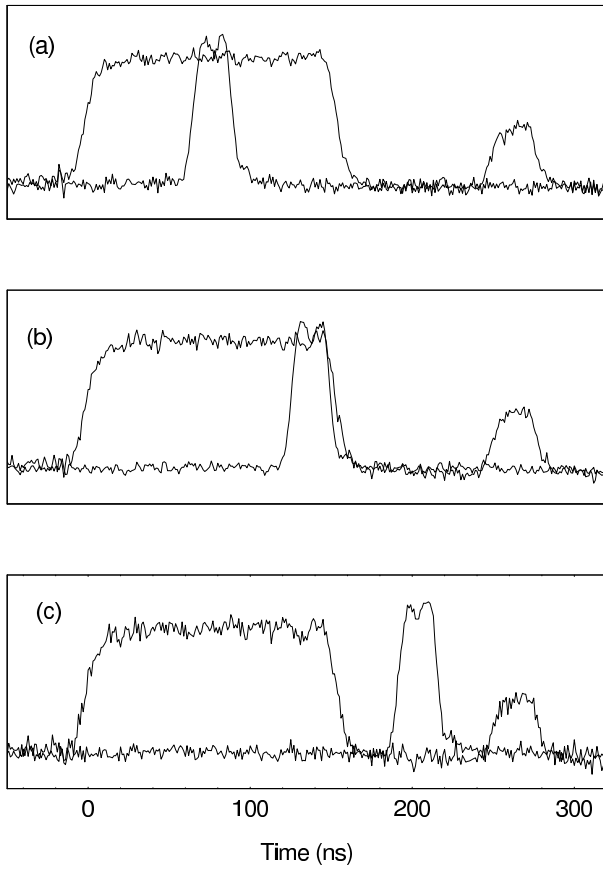


FIG. 4: Experimental pulse shapes recorded before propagation of the optical fields through the Rb cell. The noise level in these data is due to the electronics.

Sautenkov et al., “Enhancement of field generation via maximal atomic coherence..”, Fig. 4.

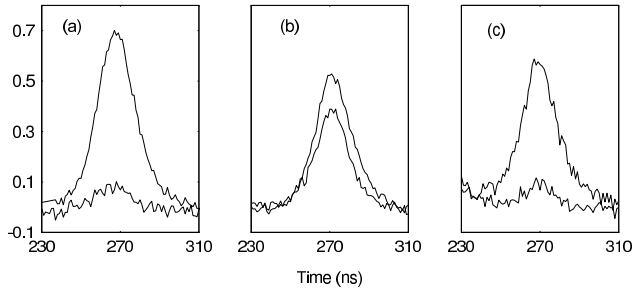


FIG. 5: Probe and generated signal fields after propagation through atomic vapor. In all figures, the probe field is stronger than the signal field. Amplitudes are normalized to amplitude of the probe pulse before entering the cell. Fig. 5b demonstrates the maximal amplitude of the generated signal field obtained by the combination of preparation pulses shown in Fig. 4b.

Sautenkov et al., “Enhancement of field generation via maximal atomic coherence..”, Fig. 5.